Molecular lines in absorption: recent results

Françoise Combes

Observatoire de Paris, DEMIRM, 61 Av. de l'Observatoire
F-75 014 Paris, France

Tommy Wiklind

Onsala Space Observatory, S-43 992, Onsala, Sweden

Abstract. Some recent results are presented about high redshift molecular absorption lines, namely about chemical abundances of elements, and in particular of water and molecular oxygen. Excitation temperatures of several molecules are found lower than the cosmic background temperature at the corresponding redshift $z = 0.88582$ in PKS1830-211, and interpretations are proposed. The radio flux monitoring of the two gravitational images of PKS1830-211 is presented over almost two years, but precise calibration is still preventing the determination of the time-delay without ambiguity. The high spectral resolution of radio observations allows to put constraints on the variation of the fine-structure constant over a large fraction of the Hubble time.

1. Molecules unobservable from the ground at $z = 0$

Because of the atmospheric absorption in the H_2O and O_2 lines, it is impossible to have a correct estimation of the abundances of theses two molecules in the local interstellar medium. The redshift allows us to get rid of the atmospheric absorption, and the highest column density line-of-sights are privileged targets to try to detect these fundamental molecules (e.g. Combes & Wiklind 1996).

1.1. Water

We have chosen the absorbing cloud in front of B0218+357, where already optically thick lines of CO, ^{13}CO and $C^{18}O$ have been detected (Combes & Wiklind 1995). The optical depth of the CO(2-1) line was derived to be 1500. The redshift is $z = 0.68466$, and the fundamental ortho transition of water at 557 GHz is redshifted to 331 GHz into an atmospheric window. An attempt to observe water in emission at $z = 2.28$ has resulted in a tentative detection (Encrenaz et al. 1993).

According to models, the H_2O/H_2 abundance ratio is expected between 10^{-7} and 10^{-5} (Leung et al. 1984, Langer & Graedel 1989). Observations of isotopic lines, such as $H_2^{18}O$ and HDO, or even H_3O^+, have confirmed these expectations. From the ground, water maser(/thermal?) emission at 183 GHz has been obtained by Cernicharo et al. (1994). However, it was thought until re-

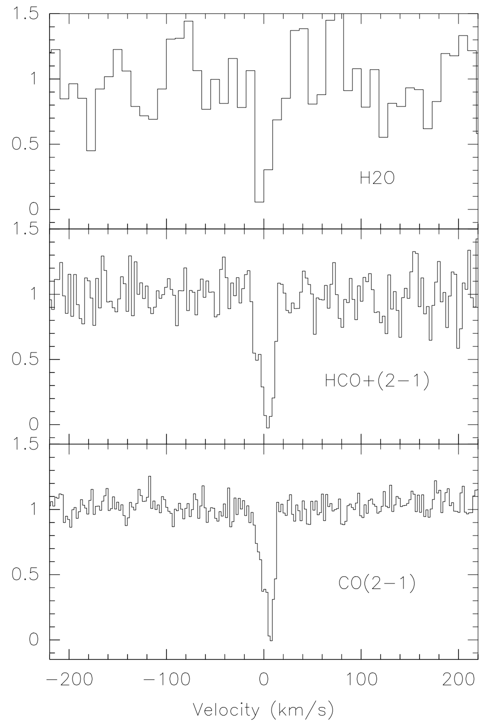

Figure 1. Spectrum of ortho–water in its fundamental line at 557 GHz, redshifted at 331 GHz, in absorption towards B0218+357. The line has the same width as the previously detected HCO^+(2–1) and CO(2–1) lines. The velocity resolution is 9.1, 2.8 and 2.2 km/s from top to bottom. All spectra have been obtained with the IRAM-30m telescope, and normalised to the continuum level completely absorbed (33% of the total).

cently that these abundances concerned only the neighbourhood of star-forming regions, such as the Orion hot core, where water ice is evaporated from grains. However, Cernicharo et al. (1997) detected with ISO water in absorption at 179μ in front of SgrB2, and this revealed that cold water was ubiquitous.

Our detection with the IRAM-30m of ortho-water in its fundamental line at 557 GHz confirms this result. The line is highly optically thick, and has about the same width as the other optically thick lines detected in absorption in this cloud (see figure 1). If the excitation temperature was high (as in the Orion hot core), we would have expected to detect also the excited line at 183 GHz (redshifted at 109 GHz). An upper limit on this line gives us an upper limit on T_{ex} of 10-15K, and an estimation of the optical depth of the 557 GHz line of $\sim$ 40 000 (Combes & Wiklind 1997). This leads to an H_2O/H_2 abundance ratio of 10^{-5}, in the upper range of expected values.

1.2. Molecular oxygen

As an element, oxygen is about twice as abundant as carbon ($O/H \sim 8.5 \cdot 10^{-4}$), meaning that at most half of the oxygen atoms can be used to make CO. The other half can be found in the form of atomic oxygen (OI), or molecules: O_2, OH and H_2O. Since OH and H_2O are much less abundant than CO, in dense molecular clouds, we expect O_2 to be about as abundant as CO. Until recently, the upper limits on the O_2/CO ratio was 0.1, from observations of the isotopic line $O^{18}O$ and the direct O_2 in emission in remote starbursts. The upper limits obtained through absorption lines are more reliable, since they involve only one individual molecular cloud, where O_2 is not photo-dissociated (O_2 is expected to be much less ubiquitous than CO).

We had already reported upper limits of $O_2/CO < 1.3 \cdot 10^{-2}$ through IRAM-30m search of the 424 GHz and 368 GHz lines (Combes & Wiklind 1995). We have improved these limits by observing the 118.7 GHz line at the Kitt Peak 12m (redshifted at 70.5 GHz), and the 56.2 GHz line at Green-Bank 43m and Nobeyama 45m (redshifted at 33.4 GHz). The new limit is $O_2/CO < 2 \cdot 10^{-3}$ at 1σ (Combes et al. 1997).

There could be several explanations to this low oxygen abundance:

- either the C/O abundance ratio in the gas phase is higher than 1. Then all the oxygen atoms are used up in the CO molecules, the O_2/CO ratio decreases exponentially with (C/O^{-1}). This means that the oxygen is frozen into grains (mainly under the form of water ice or silicates).
- the steady-state chemistry is never reached, and because of turbulence, only time-dependent models should apply (time-scales of less than $1.3 \cdot 10^5$ yr). The oxygen is therefore under the OI form, even in dense molecular clouds.
- due to chemical bi-stability, there exists two possible phases of the interstellar medium, the LIP and HIP (low and high ionization phases respectively, e.g. Le Bourlot et al. 1993, 1995). In the HIP, the O_2/CO abundance can be much lower than in the LIP. It remains to be explained why the HIP should be predominant in the ISM. Also in this model, the abundances of other elements, such as HCN or HCO^+ is not reproduced within orders of magnitude.

2. Chemical abundances

One of the aim of this work is to pinpoint evolution with redshift of the molecular abundances, which could be different from the local ones because of different element abundances, different physical environment (temperature, densities, radiation field). Many molecules have been detected at high redshift in absorption, HCO^+, HCN, HNC, CO, CS, CCH, CN, H_2O, N_2H^+, H_2CO, C_3H_2, HC_3N and isotopes; it is possible to try now a statistical comparison of abundance ratios between these detections and their analogues in the Milky Way. It is important to inter-compare absorption studies (and not emission), since there are special biases associated to each technique (absorption traces preferentially diffuse

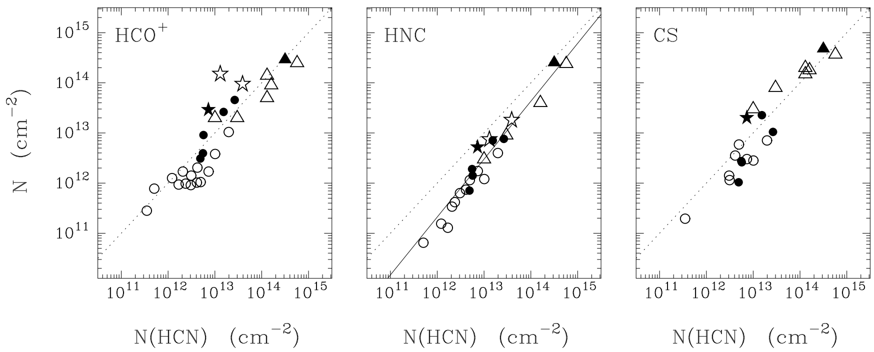

Figure 2. Column density of HCN plotted versus column densitites of HCO^+, HNC and CS. The open circles represent Galactic diffuse clouds (Lucas & Liszt 1994, 1996), filled circles represent data from Cen A (Wiklind & Combes 1997a) and open triangles represent absorption data towards SgrB2 (Greaves & Nyman 1996). The filled star represents our absorption data for PKS1413+135, open stars from B3 1504+377 at z=0.673 (Wiklind & Combes 1996b) and the filled triangle PKS1830–210 at z=0.886 (Wiklind & Combes 1996a). The full–drawn line in $N(HCN)$ vs. $N(HNC)$ is a linear fit to the data, showing how the HCN/HNC ratio increases with decreasing HCN column density.

gas). Lucas & Liszt (1994, 1996) have made a survey of molecular absorptions in front of extragalactic radio sources; they find surprising abundances, for instance HCO^+ one or two orders of magnitude larger than expected, that could be explained by turbulence-induced chemistry (Hogerheijde et al. 1995, Falgarone et al. 1995). Curiously, they find only diffuse clouds in their survey, but this might be due to a bias towards high latitudes and unobscured line-of-sights. Absorptions towards the Galactic Center (Greaves & Nyman 1996) or in CenA (Wiklind & Combes 1997a) correct this bias, in view of a comparison with high redshift absorptions (which have sometimes high column densities).

A sample of the results can be seen in figure 2, where abundances of HCO^+, HCN, HNC and CS are intercompared. The main striking point is that the high-redshift abundances are perfectly compatible with the local ones. In particular, the well known HCN/HNC variations with physical conditions is retrieved (Irvine et al. 1987). In fact, there are more variations from cloud to cloud in the Milky Way than variations due to evolution. Changes in the abundances at large distances are within the dispersion of local variations, preventing any effects of evolution to be seen.

3. Time-delay in PKS1830-211

In the previous talk, Tommy has shown how the IRAM interferometer data have confirmed that only one of the two gravitational images is absorbed by molecular clouds at the main velocity (V=0 or z = 0.88582, Wiklind & Combes 1997c).

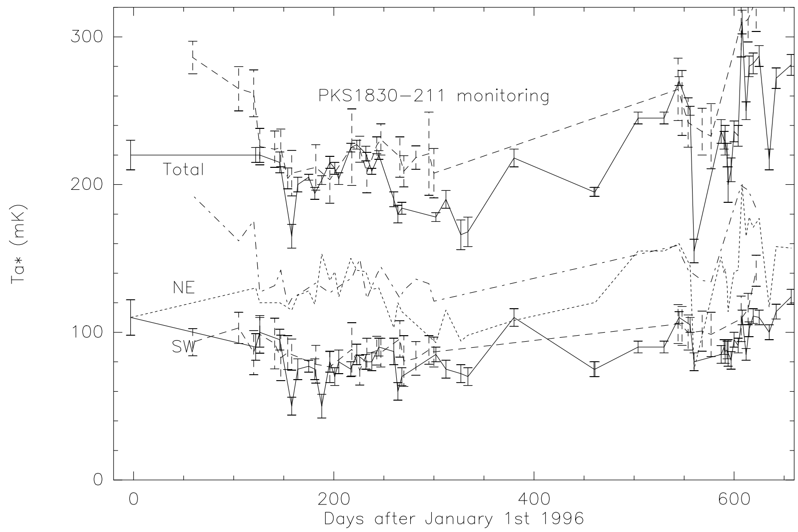

Figure 3. Results of the weekly monitoring of the quasar PKS 1830-211 in the HCO^+(2-1) line at $z = 0.88582$. The full and dashed lines represent observations done at the IRAM-30m and SEST-15m telescopes respectively. From bottom to top the curves are the measure of the continuum level successively of image B, A and total. An intrinsic level increase appears from 1996 to 1997, in the two images.

The SW image is entirely covered at V=0, which is also compatible with the BIMA data (Frye et al. 1997), while the NE image is absorbed by clouds at V $\sim$ -150km/s (may be only partially). Since the absorption at V=0 is optically thick, its depth is a good indicator of the continuum level of the SW image, while the total continuum detected with a single dish (without resolving the two images) is a measure of the sum of the NE+SW continuum levels. By a single observation, it is therefore possible to derive separately the continuum of both images. Through a monitoring of the source in its HCO^+(2-1) absorption, we can derive the light curves of the NE and SW images, and try to determine the time-delay.

We have carried out a weekly monitoring since the beginning of 1996 with the IRAM-30m and SEST-15m telescopes, the results are plotted in figure 3. The SEST data have been normalised to be compared with the IRAM ones, both are pretty compatible. However, it is difficult to derive precisely the time-delay, since the intrinsic variations of the quasar have not been of high amplitude 1996-7, and the atmospheric calibrations introduce unwanted noise in the light curves. The expected time-delay is of the order of a few weeks. Another caveat, in view of determining the Hubble constant, is that a second lens at $z = .19$ could add some amplification or shearing effect (Lovell et al. 1996).

4. Cosmic background temperature

When the absorption occurs in relatively diffuse gas, where the density is not enough to excite the rotational ladder of the molecules, the excitation temperature is close to the cosmic background temperature T_{bg}, and could be a way to check its variation with redshift. This is the case of the gas absorbed in front of PKS1830-211, where $T_{ex} \sim T_{bg}$ for most of the molecules. The measurement of T_{ex} requires the detection of two nearby transitions. When the lower ones is optically thick, only an upper limit can be derived for T_{ex}. Ideally, the two transitions should be optically thin, but then the higher one is very weak, and long integration times are required.

The results obtained with the SEST-15m and IRAM-30m are plotted in figure 4. Surprisingly, the bulk of measurements points towards an excitation temperature lower than the background temperature at $z = 0.88582$, i.e. T_{bg}= 5.20K. This could be due to a non-LTE excitation. In fact, the excitation temperature is not the same for each couple of levels considered. If the effect of collisional excitations could be neglected, the levels would be in radiative equilibrium with the black body at T_{bg} (the time-scale for this, of the order of A^{-1}, is less than a few years years for all molecules). But collisions tend to excite the lower levels at a higher temperature (since $T_{kin} > T_{bg}$). The competition between the two processes is traced by the C/A ratio (collisions versus spontaneous rates), which is non-negligible only for the first level, at low density. This will populate the $J = 1$ level a little bit higher with respect to the $J = 0$ than expected from radiative equilibrium at T_{bg}. The consequence is that the T_{ex}(1-0) will be higher than T_{bg} but T_{ex}(2-1) will be lower than T_{bg}. Since the T_{ex} measured in figure 4 do not involve the fundamental levels (the corresponding transitions, in the cm domain, would be optically thick), this could be the explanation. A detailed non-LTE model should be built to confirm this hypothesis.

5. Variation of fine-structure constant

The high spectral resolution of heterodyne techniques, the narrowness of absorption lines and their high redshift make these measurements favorable to try to refine the constraints on the variation of coupling constants with cosmic time, variations that are predicted by for instance the Kaluza-Klein and superstring theories. By comparing the HI 21cm line (Carilli et al. 1992, 1993) with rotational molecular lines, one can constrain the variations of $\alpha^2 g_p$, α being the fine-structure constant, and g_p the proton gyromagnetic ratio. Also, by intercomparison of rotational lines from different molecules, one can test the invariance of the nucleon mass m_p, since the frequencies are affected by centrifugal stretching.

Recent works on these lines have considerably improved the previous limits (e.g. Potekhin & Varshalovich 1994). By comparing various optical/UV lines (of H_2, HI, CI, SiIV) in absorption in front of quasars, Cowie & Songaila (1995) constrained the variation of $\alpha^2 g_p m_e/m_p$ to 4 $\cdot 10^{-15}$/yr. Varshalovich et al. (1996) from radio lines come to a limit of variation of $\alpha^2 g_p$ of 8 $\cdot 10^{-15}$/yr. Drinkwater et al. (1997) by a more careful analysis of the same data conclude to

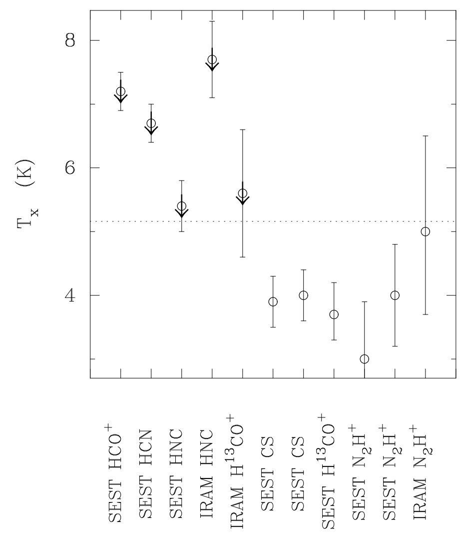

Figure 4. Measure of the excitation temperatures for several molecules shown in abcissa, from two of their rotational transitions. When the lower transition is optically thick, only an upper limit is derived. The horizontal dash line is the cosmic background temperature expected from the big-bang at the redshift of the absorber for PKS1830-211, i.e. $z = 0.88582$.

$5 \cdot 10^{-16}$/yr. We have also derived a limit from PKS1413+135 and PKS1830-211 data of $\Delta z/(1+z) < 10^{-5}$, which yield a corresponding limit of $2 \cdot 10^{-16}$/yr (Wiklind & Combes 1997b). However, geophysical constraints are in fact superior to all astrophysical ones. Damour et al. (1997) have recently come up with a limit of $5 \cdot 10^{-17}$/yr on α from the natural fission reactors which operated about $2 \cdot 10^{9}$yr ago at Oklo (Gabon). These results were obtained through analysis of the neutron capture cross section of Samarium, in the Oklo uranium mine.

Notice that we have reached an intrinsic maximum of precision with the astrophysical technique, since the limitation comes from the hypothesis that the various lines compared come from the same material, at exactly the same Doppler velocity along the line-of-sight. This hypothesis is obviously wrong when comparing HI and molecular lines; it is also wrong while intercomparing molecules, or even within lines of the same molecule, since opacity depends on excitation conditions which vary along the line of sight for each transition.

References

Carilli, C.L., Perlman E.S., Stocke J.T. 1992, ApJ 400, L13

Carilli, C.L., Rupen, M.P., Yanny, B. 1993, ApJ 412, L59

Cernicharo, J., González–Alfonso, E., Alcolea, J., Bachiller, R., & John, D. 1994, ApJ 432, L59

Cernicharo, J., et al. 1997, A&A 323, L25

Combes, F., Wiklind T. 1995, A&A 303, L61

Combes F., Wiklind T., 1996, in Cold Gas at High Redshift, eds. M.N. Bremer, P. van der Werf, H.J.A. Röttgering, C.L. Carilli, Kluwer Academic Pub., p. 215

Combes, F., Wiklind T. 1997, ApJ 486, L59

Combes F., Wiklind T., Nakai N.: 1997, A&A 327, L17

Cowie L.L., Songaila A.: 1995, ApJ 453, 596

Damour T., Dyson F.: 1997, Nucl. Phys. B. in press (hep-ph/9606486)

Drinkwater M.J., Webb J.K., Barrow J.D., Flambaun V.V.: 1997, in "Structure and Evolution of the IGM from QSO Absorption Line Systems" IAP, paris, ed. P. Petitjean & S. Charlot, p.

Encrenaz P.J., Combes F., Casoli, F., Gerin, M., Pagani, L., Horellou, C.,& Gac, C. 1993, A&A 273, L19

Falgarone E., Pineau des Forêts G., Roueff E.: 1995, A&A 300, 870

Frye B., Welch W. J., Broadhurst T.: 1997, ApJ 478, L25

Greaves J.S., Nyman L.–Å., 1996, A&A 305, 950

Hogerheijde M.R., de Geus E.J., Spaans M., van Langevelde H.J., van Dishoeck E.F., 1995, ApJ 441, L93

Irvine W.M., Goldsmith P.F., Hjalmarson A.: 1987, in "Interstellar Processes", eds. D.J. Hollenbach & H.A. Thronson, Reidel Publishers, ASSL, Proceedings, p. 561

Langer, W.D., & Graedel, T.E. 1989, ApJS 69, 241

Le Bourlot J., Pineau des Forêts G., Roueff E., 1995, A&A 297, 251

Le Bourlot J., Pineau des Forêts G., Roueff E., 1993, ApJ 416, L87

Leung, C.M., Herbst, E., & Huebner, W.F. 1984, ApJS 56, 231

Lovell, J.E.J., Reynolds, J.E., Jauncey D.L., et al. 1996, ApJ 472, L5

Lucas R., Liszt H.S.: 1994, A&A 282, L5

Lucas R., Liszt H.S.: 1996, A&A 307, 237

Potekhin A.Y., Varshalovich D.A.: 1994, A&AS 104, 89

Varshalovich D.A., Panchuk V.E., Ivanchik A.V.: 1996, Astron. Lett. 22, 6

Wiklind, T., Combes, F. 1996a, Nature, 379, 139

Wiklind, T., Combes, F. 1996b, A&A 315, 86

Wiklind, T., Combes, F. 1997a, A&A 324, 51

Wiklind, T., Combes, F. 1997b, A&A in press

Wiklind, T., Combes, F. 1997c, ApJ in press